

SEDIMENT CHARACTERISTICS OF TWO CONIFEROUS AND BROADLEAF FORESTS IN KURAIYAMA, JAPAN

Diana Hapsari¹, Takeo Ohnishi² and *Masateru Senge³

¹ Postgraduate, the United Graduate School of Agricultural Science, Japan; ² Faculty of Applied Biological Science, Gifu University, Japan; ³ Laboratory of Ltd. Union, Gifu University, Japan

*Corresponding Author, Received: 28 Dec. 2020, Revised: 22 Feb. 2021, Accepted: 07 Mar. 2021

ABSTRACT: The aim of this study was to compare the sediment characteristics of two small forest catchments, artificial coniferous (AC) and natural broadleaf (NB), utilizing sediment rating curves (SRCs) through the suspended load and hysteresis loops. The SRC equation was derived from the relationship between the water discharge value (Q) with the suspended sediment concentration (SS) or the suspended load (L) data from the recorded rainfall events. The erosivity index of AC was found to be higher than that of NB (a -values of 7.30 and 1.20 for AC and NB, respectively), showing that the erosion in the coniferous forest was greater than that in the broadleaf forest. AC also had a positive erosivity power (b -value) of 0.57, while NB had a negative value of -0.186. However, even though the b -value for NB is negative, it is close to 0. This means that even if the discharge increases, the suspended sediment concentration does not change enough to make the relationship between Q and SS for NB very low. Both catchments generated a weak coefficient of determination (R^2). Nevertheless, it seems that there is a correlation between the R^2 values and the hysteresis loops, where the weaker the R^2 , the wider the hysteresis loop can be captured. The suspended sediment of NB was finer and darker than that of AC, representing richer organic matter. The richer nutrients of NB catchment may have been brought about by the greater amount of leaf litter that flowed down due to heavy rainfall events, leading to sediment of a darker color. It was concluded that coniferous forest catchment tended to be more erosive than broadleaf forest catchments.

Keywords: Sediment rating curve, Sediment-discharge relationship, Soil erosion, Suspended sediment

1. INTRODUCTION

After World War II, the construction of wooden houses increased in Japan. Many natural broadleaf trees were cut down, and coniferous trees were planted to meet the demand for building materials. As time went by, the activity of importing timber from overseas increased due to the lower price. Thus, the coniferous plantations in Japan were gradually left unattended. As a result, many of these coniferous plantations were not well preserved or managed, triggering high erosion rates.

Vegetation cover is one of the main factors in controlling soil erosion in mountainous areas [1]. When vegetation is cleared and the ground is more exposed, there is less vegetation available to absorb energy from falling rainwater, which leads to rainfall erosion and the acceleration of erosion [2]. The type of vegetation plays a greater role in erosion than the percentage of vegetation cover, and dense forests with a high percentage of vegetation cover are seen to experience high amounts of soil loss [3]. Moreover, regardless of the density of the forest stand and the rainfall intensity, soil erosion was ranked from highest to lowest in order of Japanese cypress, Japanese cedar, and natural broadleaf forests [4].

Soil erosion in a healthy forest is known to be inhibited by the understory vegetation and the litter layer, where the smaller the litter layer, the greater the

soil erosion content [5]. On the contrary, there has not been much information on forest erosion. Many soil erosion models assume that larger canopy covers reduce the risks of erosion. Only a few erosion models assume that soil erosion can also occur under vegetation cover, depending on the height of the vegetation and water interception [6].

The sediment rating curve (SRC) is a soil erosion prediction method used by many researchers. Even though the SRC tends to underestimate the predicted total suspended load [7], it can be used to grasp the relationship among the sediment concentration (SS) or the sediment load (L), and water discharge (Q) in designated catchments. On the other hand, only a few comparative studies have been done on either soil erosion in coniferous and broadleaf forest catchments or the impact of vegetation on the SRC itself.

Therefore, the aim of this study is to compare the sediment characteristics of natural broadleaf and artificial coniferous forest catchments in the Kuraiyama Experimental Forest in Japan by utilizing sediment rating curve equations along with the suspended load and hysteresis loops of the curves.

2. METHODS

2.1 Study Area

The research was carried out at the Kuraiyama

Experimental Forest of Gifu University, located in Yamanoguchi, Hagiwara-cho, Mashita-gun, Gero City, Gifu Prefecture, in the range of 137° 12' 14" to 137° 14' 10" east longitude and 35° 58' 40" to 36° 01' 06" north latitude. The study sites are shown in Fig.1. The main focus was placed on the artificial coniferous forest catchment (AC) and the natural broadleaf forest catchment (NB). The differences between them can be found in Table 1.

Both study catchments are in the southern part of Kuraiyama Experimental Forest, with average basin slopes of 21.1° to the north. Both have streams that meander and are rocky with a three-stream order, with a catchment area of less than 10 km², as shown in Table 1. The streams are included as brooks according to the river classification [8].

The water discharge (Q) was calculated by the water depth taken from the HOBO-U20 logger measurements at the outlet with a V-shaped weir notch at three-minute intervals. The observation data used for this research were recorded from January 1st to August 19th, 2018.

The amounts of suspended sediment concentration (SS) were measured from a 1000-ml water sample using ISCO automatic water samplers. The samplers were installed at the edges of the outlets to collect water every hour during rainfall events or when the water level was above a certain height.

The water samples were filtered using glass fiber filter papers with an effective retention of 0.45 μm. The samples were then oven-dried at 150 °C for two hours and weighed to determine the mass of the sediment captured per liter of discharge. Sediment sampling was done from April 1st to September 13th,

2018.

The precipitation data were derived from a tipping bucket rain gauge installed near the NB outlet (909 m a.s.l.). Precipitation was recorded from January 1st to September 13th, 2018. A total of 24 rainfall events were recorded during the study period. Sediment sampling was conducted during only 11 of the rainfall events, the results of which are presented in Table 2.

2.2 Data Analysis

Q was derived from the overflow depth (H) through a triangular weir notch with a V-shape at the outlet channel using the following equation [9]:

$$Q = C \times H^{\frac{5}{2}} \quad (1)$$

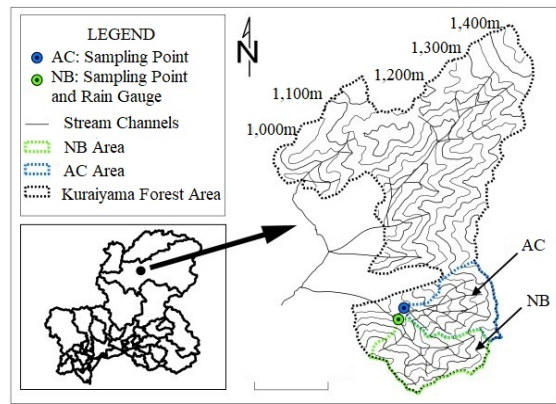


Fig.1 Research area at Kuraiyama Experimental Forest of Gifu University. The site is located around 23.5 km north from the heart of Gero City, Gifu Prefecture, Japan

Table 1 Characteristics of both study catchments

Difference	Unit	Artificial Coniferous (AC)	Natural Broadleaf (NB)
Area	km ²	0.61	0.73
Primary vegetation	-	± 75% Coniferous mix (Cedar and Cypress), 18% Quercus, 7% Thujopsis	± 77% Quercus, 13% Coniferous mix, 10% Thujopsis
Cover vegetation	-	Primary vegetation without any cover vegetation, and main vegetation covered with <i>Sasa sennanensis</i>	Primary vegetation covered by grass and fern, herbaceous, and <i>Sasa sennanensis</i>
Stream order	-	3	3
Main stream length	km	1.1	1.21
Total stream length	km	3.75	3.63
Stream type	-	Brook	Brook
Main stream slope	m km ⁻¹	0.346	0.305
Average basin slope	°	21.1	21.1
Coefficient of basin shape*	-	0.6	0.49
River density	km km ⁻²	6.29	4.98
Maximum altitude	m asl**	1278	1278
Minimum altitude	m asl**	926	909
Altitude difference	m	352	369

* Ratio between a circumference of circle with surface equal to basin area and an actual basin perimeter

** Meters above sea level

where Q is the water discharge [m^3s^{-1}] at the designated catchment, C represents the discharge coefficient, as shown by Eq.(2), and H represents the overflow water depth at the triangular weir notch [m].

$$C = 1.354 + \frac{0.004}{H} + \left(0.14 + \frac{0.2}{\sqrt{W}}\right) \left(\frac{H}{B} - 0.09\right)^2 \quad (2)$$

where W is the weir height [m] and B is the weir width [m].

To obtain the observed suspended sediment concentration (SS_o ; $mg\ l^{-1}$) and observed suspended load (L_o ; $kg\ km^{-2}\ hr^{-1}$), the following equations were used [10]:

$$SS_o = \frac{dSS}{V} \quad (3)$$

$$L_o = 3.6 \times \frac{Q \times SS_o}{A} \quad (4)$$

where dSS (mg) represents the weight of the oven-dried sediment, V (l) represents the volume of sampling water, and A (km^2) represents the catchment area.

As the observed sediment concentration could not be calculated every hour, the SRC was needed in order to predict the missing sediment concentration. The most popular equation used for the SRC employs a power function, as following equations [10,11]:

$$SS_p = a Q^b \quad (5)$$

$$L_p = c Q^{b+1} = c Q^d \quad (6)$$

where SS_p refers to the predicted suspended sediment concentration [$mg\ l^{-1}$] and L_p refers to the predicted suspended load [$kg\ km^{-2}$ per hour]. a and b are constant coefficients in the power regression derived

from Eq.(5), while c and d are those derived from Eq.(6). The actual international standard (SI) unit for a is expressed by $kg\ s^b\ m^{-(1+3b)}$, which means that a is influenced by b [10]. On the other hand, the c -value can be calculated by the following equation:

$$c = 3.6 \times \frac{a}{A} \quad (7)$$

The scatter plot of the $SS-Q$ data is attributed to the variation in sediment availability, which is called the hysteresis effect [10]. Many researchers have agreed that "a" is the erosion severity index and "b" is the erosivity power of the designated river [7, 12, 13, 14, 15].

The total predicted load (TL ; $kg\ km^{-2}$) was derived by summarizing the predicted load during the sampling period (T ; hr) [10] from January 1st to August 19th, 2018.

$$TL_p = \int_0^T L_p dt \quad (8)$$

3. RESULTS AND DISCUSSION

3.1 Runoff, Sediment Concentration, and Load

The runoff, sediment concentration, and load are compared between the coniferous and broadleaf catchments by Fig.2, Fig.3, and Fig.4, respectively.

The rainfall events are separated into two categories: higher sediment load at NB (E1, E4, E5, E6, E7, E8) and higher sediment load at AC (E2, E3, E9, E10, E11), which is plotted by the solid circle and open circle symbols respectively in these figures.

Fig.2 presents a comparison of the simultaneous water discharge between the coniferous and broadleaf forest catchments during the recorded SS sampling. In the figure, AC appears to have a higher Q during the

Table 2 Overview of recorded rainfall events and suspended sediment sampling

Event no.	Date	Total rainfall [mm]	Total runoff [mm]		Runoff ratio* [No dimensions]	
			AC	NB	AC	NB
E1	April 5 th - 7 th	52.0	8.84	7.21	0.17	0.14
E2	April 11 th - 12 th	36.0	7.35	5.46	0.20	0.15
E3	May 2 nd - 3 rd	74.0	15.21	12.03	0.21	0.16
NE1	May 10 th - 11 th	0.0	6.43	7.40	-	-
E4	May 18 th - 19 th	30.5	3.41	3.36	0.11	0.11
E5	June 8 th -9 th	34.0	2.84	2.38	0.08	0.07
E6	June 19 th - 21 st	54.5	6.35	5.07	0.12	0.09
E7	June 26 th - 28 th	81.0	16.61	13.45	0.21	0.17
NE2	July 13 th - 14 th	0.0	6.16	7.40	-	-
E8	July 15 th	27.5	2.33	1.76	0.08	0.06
E9	Aug. 12 th - 13 th	40.0	2.89	1.79	0.07	0.04
E10	Aug. 13 th	15.5	1.60	0.80	0.10	0.05
E11	Aug. 15 th - 17 th	127.5	36.91	20.05	0.29	0.16

NE: Non-rainfall events for which runoff was high and sediment sampling could be conducted.

*Runoff ratio was calculated from the total runoff divided by total rainfall.

high discharge flow (66 data set), while NB has a higher Q during the low discharge flow (32 data set). Furthermore, AC is seen to reach higher discharge peaks compared to NB. It is correlated with the runoff ratio presented in Table 2, where AC has greater on both total runoff and the runoff ratio.

On the contrary, Fig.3 shows that the suspended sediment concentrations (SS) are almost the same between the two catchments, even though the discharge was increasing. The suspended sediment concentration of 47 data sets are higher at NB than AC, while 51 data sets show that the sediment concentration at AC is higher than NB. Since the runoff ratio is higher for AC, the observed suspended loads are higher for AC (Fig.4). The suspended load of 67 data sets were higher at AC than NB during the rainfall events.

Water discharge has a positive relationship with rainfall [13]. When the rainfall intensity increases, the water discharge also increases. With longer rainless periods come more sediment being stored on the bed (available sediment). The energy required to make the sediment move downstream is low during the rainless period, so it settles down onto the bed and becomes available to be transported soon after the next rainfall starts. When the rainfall comes, the energy increases, and it is enough to transport the available sediment in the high-water discharge.

Based on Fig.4, it can be concluded that the relationship between $L-Q$ is positive in this study, where the higher the discharge flow, the greater the amount of suspended sediment that can be transported. This leads to higher suspended loads.

3.2 SS- Q Relationship and Hysteresis Loops

The suspended sediment transported in a river commonly represents a mixture of sediment derived from different locations and sources within the specific catchment [16]. The mixture of the captured sediment represents the runoff energy function, and the changes in the sediment supply and the depletion process of the designated catchment [8] are described by hysteresis loops [17]. There are five major types of loops representing the $SS-Q$ relationship: single straight line, single straight line with a loop, clockwise, counter-clockwise, and figure-8 loops [12, 17].

However, only three types of loops were found in this study, namely, clockwise, figure-8, and single straight line.

Fig. 5 presents a sample of the loops at E1, E3, and E4. The hysteresis loops at E1 represent clockwise loops at both catchments. Clockwise loops are found at both catchments at E1 and E2. The loops represent the amount of sediment available from the previous rainfall event (before E1), which was depleted soon after the next rainfall (E1) began, then

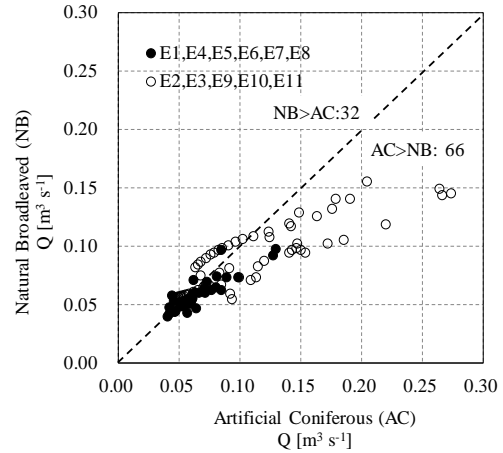


Fig.2 Comparison of water discharge (Q) between artificial coniferous (AC) and natural broadleaf (NB) forests during sediment sampling

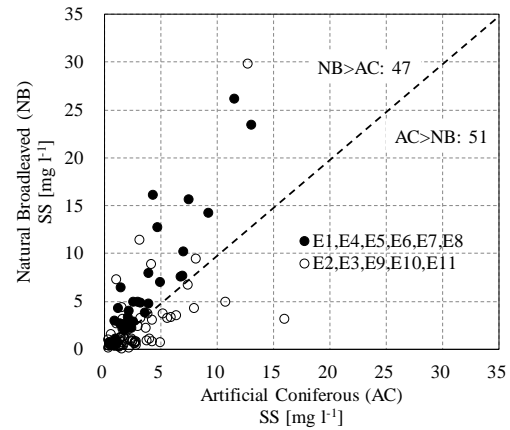


Fig.3 Comparison of simultaneously observed suspended sediment concentration in artificial coniferous (AC) and natural broadleaf (NB) forests

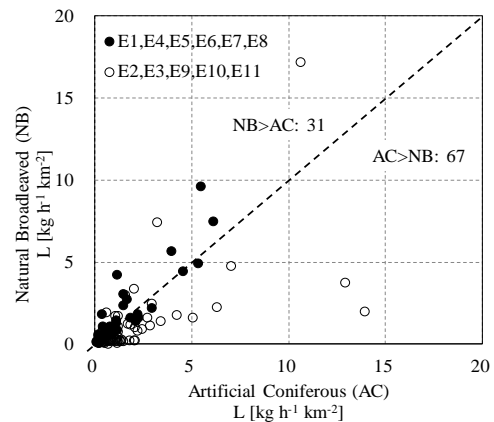


Fig.4 Comparison of simultaneously observed suspended sediment load in artificial coniferous (AC) and natural broadleaf (NB) forests

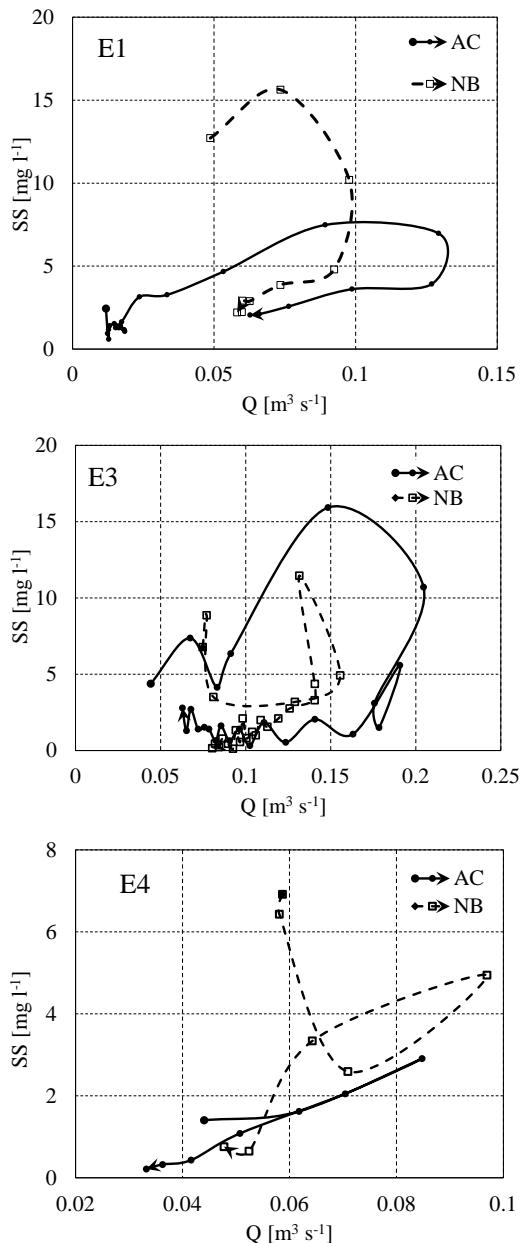


Fig.5 SS-Q hysteresis loops in AC and NB during E1 (above), E3 (middle) and E4 (below)

exhausted before the falling discharge stage. This means that the mechanism of sediment supply and depletion was progressive before the peak discharge [18].

E3 presents the figure-8 loops that can be found at both catchments also at E4, E7, and E11. These loops often occur when there are two or more discharge peaks for one rainfall event. The more discharge peaks that occur during one event, the more complicated the loops are.

However, E4 presents different loops between AC and NB, where both of them are seen to have a single discharge peak. A single straight line occurs in AC. This shows that the sediment increased and decreased

in pace with the discharge, making the same amount of SS at the same Q during the rising and falling stages.

On the other hand, the figure-8 loop of NB at E4 represents two sediment sources during one event. Firstly, available sediment was in the river before E4 had started and was depleted soon after the E4 rain started, and then exhausted before the Q peak. Secondly, after the available sediment was exhausted, the sediment flowing in the river due to the rainfall (direct sediment) led to the second SS peak, which caused the figure-8 loop [19].

Hysteresis loops are useful tools for identifying the different processes causing the relationship between Q and SS [20]. However, when an event has a complicated hysteresis loop (as recorded at E11), a hysteresis interpretation cannot be easily made.

3.3 Sediment Rating Curve (SRC)

Sediment Rating Curves derived from the relationship between the water discharge value (Q) with the suspended sediment concentration (SS) or the suspended load (L) are presented in Fig. 6. The catchments are seen to have distinct c -values of 43.1 and 5.91 for AC and NB, respectively, making the a -values different (7.30 and 1.20, respectively). Since a is the erosion severity index of the catchment, it can be concluded that erosion in the coniferous catchment is greater than that in the broadleaf catchment.

The b -values present different relationships between the two catchments. AC has a positive b -value (0.57), while NB has a negative value (-0.186). However, the d -values are 1.57 and 0.814 for AC and NB, respectively. The positive value for the erosivity power shows that when the discharge increased, the suspended sediment concentration being transported also increased, where the higher the discharge, the greater the suspended load that could be transported. On the contrary, even though the b -value for NB is negative, it is close to 0. This means that even if the discharge increased, the suspended sediment concentration did not change enough to make the relationship between Q and SS for NB very low. It can be concluded that the coniferous catchment had greater erosivity than the broadleaf catchment.

The SRCs produced from the two catchments showed a poor relationship between the water discharge and the suspended load. Both catchments generated weak coefficients of determination. The low accuracy of the SRCs was due to the large scatter in the data brought about by the variation in data caused by the SS- Q hysteresis loops.

Even though the R^2 on the L - Q lines in the figure is low, the difference between the two catchments is understood. The Q value at the intersecting point between the two rating curve lines shows $0.072 \text{ m}^3\text{s}^{-1}$. This means that before the water discharge reached $0.072 \text{ m}^3\text{s}^{-1}$, the broadleaf catchment was more erosive than the coniferous catchment. Nevertheless,

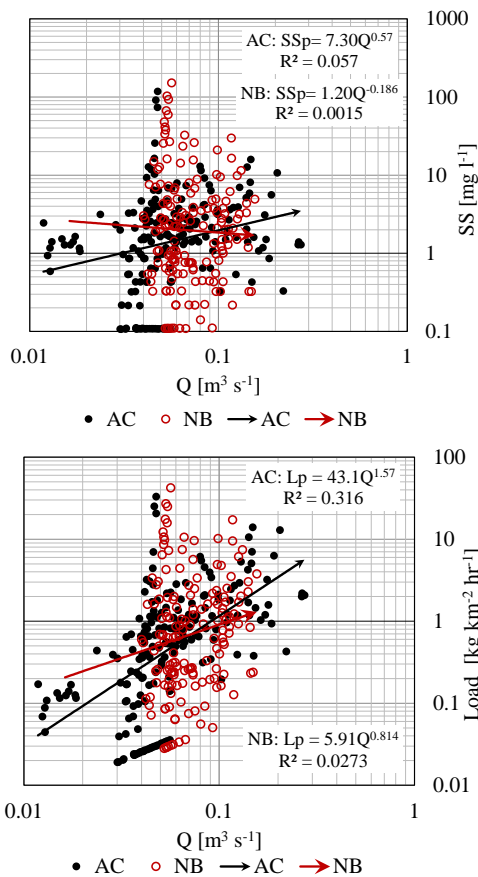


Fig.6 Sediment Rating Curves (SRC) in artificial coniferous (AC) and natural broadleaf (NB) catchments: SS-based (above) and load-based (below)

Table 3 Predicted suspended load generated from SRC at artificial coniferous (AC) and natural broadleaf (NB) catchments

Month	Load [kg km ²]		Rainfall (mm)
	AC	NB	
January	172.6	200.4	165.0
February	3.2	59.6	29.0
March	762.2	489.1	298.5
April	712.4	416.3	342.5
May	213.6	352.3	309.0
June	1202.0	284.9	476.5
July	2943.0	752.7	892.0
August*	123.9	105.9	184.6
Total	6132.9	2661.2	2668.1

*) Sampling was conducted until August 19th

the coniferous forest catchment became more erosive than the broadleaf forest catchment after the discharge levels reached 0.072 m³s⁻¹. This condition confirms that NB had a higher base flow, making the available stored sediment greater than that of AC. In comparison, AC had greater sediment transfer power with higher discharge during rainfall events.

Furthermore, a correlation is seen between the R² values and the hysteresis loops. NB is seen to have a weaker coefficient than AC; and yet, the hysteresis loops are wider for NB than for AC (Fig. 5). It is presumed that the sediment for NB mostly came from the available sediment, which was transferred soon after the rainfall began and exhausted before the discharge peak. On the contrary, AC is seen to have lower available sediment, and its source mostly depended on direct sediment during rainfall events and increased when the discharge increased.

3.4 Load Prediction

Even though the suspended loads generated from the SRCs were more underestimated than the observed suspended loads [7, 21, 22], and tended to underestimate the SS during high discharge flow and to overestimate the SS during low discharge flow [15, 23], the monthly sediment load continued to be calculated as shown in Table 3. The total predicted loads were 6.13 and 2.66 tonnes km⁻² per sampling period (January 1st to August 19th, 2018) for AC and NB, respectively.

It can be concluded that the coniferous forest had greater suspended sediment loss mainly due to the higher runoff ratio of coniferous forest compared to broadleaf forest as shown in Table 2. The highest soil erosion rate was at the Japanese cypress stand without any understory vegetation, followed by the Japanese cypress stand with fern as the understory vegetation, the broadleaf forest stand, and the Japanese cedar stand [24].

3.5 Seasonal Difference

Based on the monthly total predicted suspended load presented in Table 3, AC had higher loads than NB. However, the observed loads and the monthly total predicted loads revealed seasonal trends.

The broadleaf catchment had higher observed loads at the beginning of spring (E1) and early summer (E4, E5, E6, E7, and E8), as seen in Fig.4. On the contrary, the coniferous catchment had higher observed loads during spring (E2 and E3) and at the end of summer (E9, E10, and E11).

The broadleaf forest catchment had higher suspended loads during winter (Jan-Feb) and the beginning of summer (May), when there were many rainless periods. On the contrary, the coniferous forest catchment had higher loads at the beginning of spring (Mar) and summer (Jun-Aug), when there were many periods of rainfall.

It is presumed that during the rainfall events, the litter in NB inhibited the runoff so that the suspended load amounts were lower than in AC. However, during the rainless periods, a higher amount of available sediment might have been quickly depleted at the beginning of a rain event and stored up again

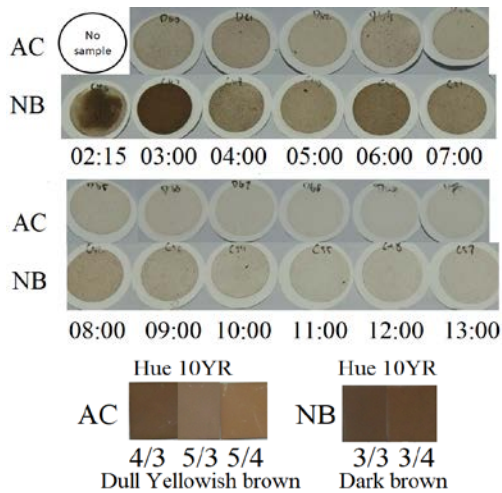


Fig.7 Suspended sediment color captured during E7 sampling period in artificial coniferous (AC) and natural broadleaf (NB) forests



Fig.8 The vegetation type at AC (above) and NB (below) in the end of autumn

after the event had ended, making the suspended load during rainless periods higher in NB.

Unfortunately, sampling could not be done until the end of the year. Thus, the presumption of factors affecting sediment cannot be discussed any further.

The most erosive rainfall events commonly occurred during the dry period (June – October),

when there were short durations of rainfall and the rainfall volume was incorporated into the soil [25]. In this study, high amounts of total predicted loads were found during June and July. The total rainfall in the study area was high from June to August, and there were many short-duration rainfall events (e.g., E5, E8, E9, and E10).

3.6 Suspension Color

The *b*-value is also related to the soil properties, such as the grain size distribution of the available material. The darker the soil, the richer the organic matter and the higher the moisture content [4]. The broadleaf forest had a lower *b*-value followed by a darker soil color (Hue 10YR $\frac{3}{4}$ dark brown) than the coniferous forest (Hue 10YR $\frac{5}{4}$ dull yellowish-brown), as shown in Fig. 7. Moreover, the sediment in the NB forest had a fine texture, while the sediment in the AC forest had a coarser texture. It is presumed that the sediment in the NB forest consisted of hummus and more organic matter. On the contrary, the sediment in the AC forest mostly consisted of soil particle fractions.

However, the difference in the *b*-values between the coniferous and broadleaf forests was not great. This means that the two soil colors were of the same level (Hue 10YR). It is supposed that vegetation and the *b*-value are correlated through the soil properties. However, further research into the relationship between vegetation and the *b*-value is needed to confirm this point.

3.7 Vegetation Factor

Understory vegetation plays the primary role in controlling soil erosion rather than the main type of vegetation [4, 25, 26, 27, 28, 29]. It enhances infiltration and prevents soil erosion, while sparse floor coverage leads to direct splash erosion and increases the overland flow [26]. That is why the increasing water discharge in the broadleaf forest was slower than that in the coniferous forest during the significant rainfall events.

Moreover, litter plays an essential role in soil erosion [5]. Some broadleaf tree species withered during the winter while coniferous stay evergreen (Fig.8). Micro terraces may have formed that slowed and spread the overland flow, enhanced infiltration, and capture and filter sediment so that the suspended sediment in the NB forest was darker and finer than that in the AC forest. On the contrary, the coniferous leaves withered more slowly than the broadleaves [4], so that the overland flow was reduced and soil erosion occurred. The coarse texture of the suspended sediment captured in the AC forest represents the soil fraction due to the lack of organic matter from the litter of withered leaves. Unfortunately, no further

research has been done on the difference in litter between the two catchments discussed in this study.

4. CONCLUSION

Many factors were seen to affect the *Q-L* relationship in this study, including the water and sediment factors. The water factor was correlated with the precipitation intensity, areal distribution, runoff amount, and discharge rates. The suspended sediment was influenced by the temporal mobilization, storage, and sediment depletion. Moreover, the amount and texture of the sediment also influenced the relationship. The richer nutrients of the catchment may have been brought about by the greater amount of leaf litter that flowed down due to the heavy rainfall events, leading to a finer texture and darker soil color.

Furthermore, *SRC* can be used as a simple tool to describe the relationship between the suspended sediment transport and water discharge flow. Using only *SRC* in one catchment will not give much information about soil erosion. However, it can be used as a simple tool to compare two or more small catchments nearby to understand the difference between them.

5. REFERENCES

- [1] Zhang Y. and Liu B.Y., Effect of Different Vegetation Types on Soil Erosion by Water. *Acta Bot. Sin.*, Issue 10, 2003, pp. 1204–1209.
- [2] Hudson N.W., Soil Conservation. Chapter 3, The Physics of Rainfall, 2nd. ed. Batsford, London, and Cornell University Press, Ithaca, NY, 1981.
- [3] Mohammad A.G. and Adam M.A., The Impact of Vegetative Cover Type on Runoff and Soil Erosion under Different Land Uses. *Catena*, Vol. 81, Issue 2, 2010, pp. 97–103.
- [4] Razafindrabe B.H.N., He B., Inoue S., Ezaki T., and Shaw R., The Role of Forest Stand Density in Controlling Soil Erosion Implications to Sediment-related Disaster in Japan. *Environ. Monit. Assess.*, Issue 160, 2010, pp. 337–354.
- [5] Wakahara T., Ishikawa Y., Shiraki K., Todo H., Miya T., Kataoka F., Suzuki M., and Uchiyama Y., Seasonal Changes in the Amount of Litter Layer and Soil Erosion in the Forest Floor – an Impoverished Understory by Deer Impact at Doudaira, Tanzawa Mountains. *Proceedings 4th International Conference on Scour and Erosion (ICSE-4)*, November 5-7, 2008, Tokyo, Japan. The Japan Geotechnical Society, 2008, pp. 628 – 633.
- [6] Selkimaki M., Gonzales-Olabarria J.R., and Pukkala T., Site and Stand Characteristic Related to Surface Erosion Occurrence in Forest of Catalonia, Spain. *Eur. J. Forest Res.*, Issue 131, 2012, pp. 727 – 738.
- [7] Asselman N.E.M., Fitting and Interpretation of Sediment Rating Curves. *J. Hydrol.*, Issue 234, 2000, pp. 228–248.
- [8] Chapman D., *Water Quality Assessments-A Guide to Use of Biota, Sediments, and Water in Environmental Monitoring-Second Edition*. E&FN Spon: Cambridge. Editor, 1992.
- [9] Japan Society of Civil Engineers, *Hydraulic formulary*, 1971, pp. 111-112. (in Japanese)
- [10] Warrick J.A., Trend Analyses with River Sediment Rating Curves. *Hydrological Processes.*, Issue 29, 2014, pp. 936 – 949.
- [11] Ide J., Kume T., Wakiyama Y., Higashi N., Chiwa M., and Otsuki K., Estimation of Annual Suspended Sediment Yield from a Japanese Cypress (*Chamaecyparis obtuse*) Plantation Considering Antecedent Rainfalls. *Forest Ecology and Management*, Issue 257, 2009, pp. 1955-1965.
- [12] Hapsari D., Onishi T., Imaizumi F., Noda K., and Senge M., The Use of Sediment Rating Curve under its Limitation to Estimate the Suspended Load. *Reviews in Agricultural Science*, Issue 7, 2019, pp. 88-101.
- [13] Baca P., Hysteresis Effect in Suspended Sediment Concentration in the Rybarik Basin, Slovakia. *Hydrolog. Sci. J.*, Issue 53, 2008, pp. 224–235.
- [14] Walling D.E., Limitation of Rating Curve Technique for Estimating Suspended Sediment Loads, with Particular Reference to British River. *Erosion and Solid Matter Transport in Inland Waters*, IAHS Publ., Issue 122, 1977, pp. 34–48.
- [15] Horowitz A.J., Determining Annual Suspended Sediment and Sediment-Associated Trace Element and Nutrient Fluxes. *Science of the Total Environment*, Issue 400, 2008, pp. 315–345.
- [16] Carter J., Owens P.N., Walling D.E., and Leeks G.J.L., Fingerprinting Suspended Sediment Sources in a Large Urban River System. *Sci. Total Environ.*, Issue 314–316, 2003, pp. 513–534.
- [17] Williams G.P., Sediment Concentration Versus Water Discharge During Single Hydrological Events in Rivers. *J. Hydrol.*, Issue 111, 1989, pp. 89–106.
- [18] Sadeghi S.H.R., Mizuyama T., Miyata S., Gomi T., Kosugi K., Fukushima T., Mizugaki S., and Onda Y., Development, Evaluation and Interpretation of Sediment Rating Curves for a Japanese Small Mountainous Reforested Watershed. *Geoderma*, Issue 148, 2008, pp. 198–211.
- [19] Whittaker A.C., Attal M., Cowie P.A., Tucker G.E., and Roberts G., Decoding Temporal and Spatial Patterns of Fault Uplift Using Transient River Long Profiles, *Geomorphology*, Issue 100, 2008, pp. 506–526.
- [20] Gao P. and Josefson M., Event-based Suspended Sediment Dynamic in a Central New York

- Watershed. Geomorphology, Issue 139–140, 2012, pp. 425–437.
- [21] Heng, Sokchhay and Suetsugi T., Development of a Regional Model for Catchment-Scale Suspended Sediment Yield Estimation in Ungauged Rivers of the Lower Mekong Catchment. Geoderma, Issue 235-236, 2014, pp. 334–346.
- [22] Girolamo A.M., Pappagallo G., and Porto A.Lo., Temporal Variability of Suspended Sediment Transport and Rating Curves in a Mediterranean River Catchment: The Celone (SE Italy). Catena, Issue 128, 2015, pp.135–145.
- [23] Boukhrissa Z.A., Khanchous K., Bissonnais Y.L., and Tourki M., Prediction of Sediment Load by Sediment Rating Curve and Neural Network (ANN) in El Kebir Catchment, Algeria. J. Earth. Syst. Sci., Volume. 122, Issue 5, 2013, pp. 1303–1312.
- [24] Wakiyama Y., Onda Y., Mizugaki S., Asai H., and Hiramatsu S., Soil Erosion Rates on Forested Mountain Hillslopes Estimated Using ^{137}Cs and $^{210}\text{Pb}_{\text{ex}}$. Geoderma, Issue 159, 2010, pp. 39–52.
- [25] Gimenez R., Casali J., Grande I., Diez J., Campo M.A., Alvarez-Moroz J., and Goni M., Factors Controlling Sediment Export in a Small Agricultural Watershed in Navarre (Spain). Agric. Water Manag., Issue 110, 2012, pp. 1–8.
- [26] Miyata S., Kosugi K., Gomi T., and Mizuyama T., Effect on Forest Floor Coverage on Overland Flow and Soil Erosion on Hillslopes in Japanese Cypress Plantation Forest. Water Resour. Res., Issue 45, 2009, pp. 1–17.
- [27] Miura S., Yoshinaga S., and Yamada T., Protective Effect of Floor Cover Againsts Erosion on Steep Slopes Forested with *Camaecyparis Obtusa* (hinoki) and Other Species. J. For. Res., Issue 8, 2003, pp. 27–35.
- [28] Ayed M.G. and Adam M.A., The Impact of Vegetative Cover Type on Runoff and Soil Erosion Under Different Land Uses. Catena, Volume 81, Issue 2, 2010, pp. 97–103.
- [29] Wang J., Ishidara H., Sun W., and Ning S., Development and Interpretation of New Sediment Rating Curve Considering the Effect of Vegetation Cover for Asia Catchment. The Scientific World Journal, 2013.

Copyright © Int. J. of GEOMATE. All rights reserved, including the making of copies unless permission is obtained from the copyright proprietors.
